PHYSICAL REVIEW B **69**, 054112 (2004)

Structural and electronic properties of Si_3P_4

M. Huang, Y. P. Feng,* and A. T. L. Lim
Department of Physics, Faculty of Science, National University of Singapore, 2 Science Drive 3, Singapore 117542

J. C. Zheng
Center for Data Intensive Computing, Brookhaven National Laboratory, Upton, New York, 11973, USA

(Received 18 July 2003; published 27 February 2004)

Structural and electronic properties of Si_3P_4 were investigated using first-principles total-energy method based on density-functional theory and the local-density approximation (LDA). It was found that pseudocubic-Si_3P_4 is energetically favored relative to other phases of Si_3P_4 considered in this study. All phases of Si_3P_4 have low bulk moduli, with the γ phase being the hardest (110 GPa). Furthermore, band-structure and density-of-states calculations reveal that α, β_1, pseudocubic, and graphitic phases of Si_3P_4 are semiconducting while β_2, cubic, and γ phases are metallic within LDA. Correction of LDA energy band gap by a more accurate method will likely result in Si_3P_4 being a narrow gap semiconductor. The structural and electronic properties of Si_3P_4 are compared with those of similar compounds, i.e., C_3N_4, Si_3N_4, Ge_3N_4, and C_3P_4.

DOI: 10.1103/PhysRevB.69.054112 PACS number(s): 61.50.Ah, 71.20.−b, 61.66.−f, 62.20.−x

INTRODUCTION

Amorphous Si and Si-based semiconducting alloys are of considerable technological importance in a wide variety of applications in the micro- and opto-electronic devices, such as heterojunction bipolar transistors, photovoltaic solar cells, sensors, and light-emitting diodes.[1,2] In particular, amorphous Si-group-III or -V alloys have attracted wide interest. This is due to the fact that group-III and group-V elements play the roles of both dopants and terminators of Si dangling bonds.[3] Moreover, the physical properties of these alloys can be tailored by changing their composition.[4] Recent advances in silicides as contacts and interconnects in microelectronic devices and as active layers in sensors have motivated the search for new silicides.[5]

During the last two decades, thermal stability, crystallization, and optical properties of amorphous Si:P alloy thin films have been studied,[4–7] and both optical and electrical investigations of $Si_{1-x}P_x$ alloy thin films have been carried out.[8] The structures and energetics of a few silicon-phosphorus compounds were studied by using the *ab initio* molecular-orbital method by Baboul *et al.*[9] It was found that there exist mainly two types of crystallization products of the thin film, i.e., Si and silicon phosphide.[4,8] Furthermore, the optical band gap of the Si:P alloy thin film can be tailored within a range of 1.5–2.15 eV by varying the P concentration (with 20–44 %) and annealing temperature.[7] The optical band gap of a newly found silicon phosphide, $Si_{12}P_5$, which was discovered during the initial crystallization studies of amorphous Si-P alloys, is 1.55 ± 0.08 eV.[5] Based on these results, crystalline Si_3P_4 can be expected to be a semiconductor with a sizable band gap.

In this study, we investigate the structural and electronic properties of Si_3P_4 using first-principles total-energy calculation based on the density-functional theory (DFT).[10,11] DFT has been very successful in predicting crystal structures and properties of materials and has been widely used in theoretical studies of similar materials such as Si_3N_4,[12] C_3N_4,[13] Ge_3N_4,[14,15] and C_3P_4.[16] It is used here to determine the structural and electronic properties of Si_3P_4 and to explore its potential applications.

COMPUTATIONAL DETAILS

To our knowledge, there has not been any experimental investigation on the crystal structure of Si_3P_4. Therefore we begin with the possible configurations of Si_3N_4 and C_3N_4 as suggested in Refs. 12 and 13 with N substituted by P and with C substituted by Si. The structures considered include α-Si_3P_4, two β phases (β_1 with space group $P6_3$ and β_2 with space group $P6_3/m$), cubic-, cubic spinel-(γ-Si_3P_4), pseudocubic-, and graphitic-Si_3P_4. In this study, we only considered several silicon phosphide structures with the stoichiometry Si_3P_4. Other stoichiometries such as $Si_{12}P_5$, SiP, and SiP_2 have also been found experimentally but are not considered in the present study.[4–6,8]

First-principles total-energy calculations were performed using the CASTEP code.[17,18] The local-density approximation (LDA) for exchange-correlation effects and the Vanderbilt ultrasoft pseudopotentials[19] were used in the calculations. The electron wave functions were expanded into plane waves up to a cutoff energy of 310 eV. Special k points generated according to the Monkhorst-Pack scheme[20] were used for integration over the irreducible wedge of the Brillouin zone of the various structures. We used 18 k points for α-Si_3P_4, 36 for both β_1- and β_2-Si_3P_4, 32 for cubic-, γ-, pseudocubic-, and graphitic-Si_3P_4. Good convergence is achieved with this cutoff energy and the number of k points for the various Si_3P_4 structures considered. Each structure is optimized under the preselected symmetry. The geometric relaxation is converged to within 0.05 eV/Å for root-mean-square force per atom, 0.10 Gpa for root-mean-square stress, and 0.001 Å for root-mean-square ionic displacement. Similar calculations were also carried out on α-, β-, and γ-Si_3N_4, to facilitate direct comparison with previous studies. The results of these calculations are found to be in ex-

TABLE I. Calculated equilibrium structural parameters and properties of various phases of Si_3P_4.

Structure	Pseudocubic	γ	α	Cubic	β_1	β_2	Graphitic
Space group	P-42m (111)	Fd-3m (227)	$P3_1c$ (159)	I-43d (220)	$P6_3$ (173)	$P6_3/m$ (176)	P-6m2 (187)
Lattice parameter (Å)	$a=4.961$ $c=4.978$	$a=9.701$	$a=9.481$ $c=6.877$	$a=7.879$	$a=9.570$ $c=3.566$	$a=9.549$ $c=3.618$	$a=6.969$ $c=8.584$
B (GPa)	91	110	67	63	75	76	
Density (g/cm^3)	2.822	3.030	2.583	2.827	2.444	2.420	1.915
E_0 (eV/Si_3P_4 unit)	-1047.79	-1047.24	-1046.97	-1046.70	-1046.42	-1046.28	-1044.09
LDA band gap (eV)	0 (ind)		0.169 (dir)		0.082 (ind)		0.983 (dir)

cellent agreement with those of previous first-principles studies on these materials.

RESULT

The equilibrium structural parameters, bulk modulus, and total energy per Si_3P_4 unit for the various phases considered are summarized in Table I. The calculated total energy per Si_3P_4 unit as a function of volume is shown in Fig. 1 for each of the seven structures. It is clear that unlike Si_3N_4, pseudocubic-Si_3P_4 is energetically favored relative to the other phases. The total energy of pseudocubic-Si_3P_4 is lower than that of the next most stable phase, i.e., γ-Si_3P_4 by about half an eV per Si_3P_4 unit. The calculated atomic positions of these two phases (pseudocubic and γ) are listed in Table II, and models of pseudocubic- and γ-Si_3P_4 structure are shown in Fig. 2. Due to its layered structure, the graphitic phase has the largest equilibrium volume per Si_3P_4 unit or lowest density, and is the least energetically favored structure among the seven phases considered. We also found that the internal coordinates of α-Si_3P_4 and the two β-phases of Si_3P_4 are strongly driven by relaxation. Compared to the positions of Si and N atoms in α- and β-Si_3N_4, the Si and P atoms are significantly displaced in α- and β-Si_3P_4. It is likely that these phases of Si_3P_4 are unstable. To further assess the mechanical stability of pseudocubic-Si_3P_4, we further relaxed the structure without the space group constraint from the previously optimized coordinates. Virtually no further changes in the structural parameters, internal coordinates and total energy were observed. As the pseudocubic phase is a type of defect zinc-blende structure, structural optimization of this phase was also carried out beginning from the ideal zinc-blende coordinates without symmetry constraint. The final structures obtained using different initial atomic coordinates are essentially the same. Hence we conclude that the pseudocubic structure is both energetically and mechanically stable.

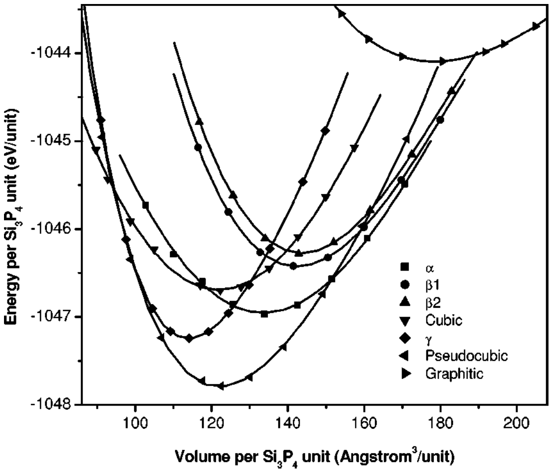

FIG. 1. Calculated total energy per Si_3P_4 unit as a function of volume for the various structures investigated. The calculated data points are fitted to the Murnaghan equation of state to obtain the bulk modulus for each structure.

To estimate the bulk modulus, we assumed uniform compression and expansion of the lattice and calculated the total crystal energy as a function of volume for each optimized structure. At a given volume, the atomic positions were relaxed within the preselected space group. The calculated total energies for each structure are then fitted to the Murnaghan equation of state to obtain the bulk moduli. The calculated bulk moduli for the various phases of Si_3P_4 are listed in Table I. We can see that the bulk moduli are much lower than those of Si_3N_4. The γ-Si_3P_4 has the highest bulk modulus of 110 GPa because this structure contains sixfold coordinated silicon atoms.[21] The energetically most favored structure, pseudocubic-Si_3P_4, has a bulk modulus of 91 GPa.

We also calculate the band structure and density of states (DOS) for each of the seven phases of Si_3P_4. It was found that α-, graphitic-, β_1-, and pseudocubic-Si_3P_4 are semiconducting within LDA (Fig. 3), while β_2-, cubic-, and γ-Si_3P_4 are metallic (Fig. 4). As can be seen in Fig. 3, α- and graphite-Si_3P_4 have direct band gaps while β_1- and pseudocubic-Si_3P_4 show indirect band gaps. The band gap of α-Si_3P_4 is 0.169 eV and is located at the Γ point. Graphitic-Si_3P_4 has a much wider energy gap. The direct energy gap of 0.983 eV located at the A point of the first Brilloun zone is

TABLE II. The calculated atomic positions of pseudocubic- and γ-Si_3P_4.

	Pseudocubic	γ
Si_1	(0.000, 0.000, 0.000)	(0.500, 0.500, 0.500)
Si_2	(0.500, 0.000, 0.500)	(0.125, 0.125, 0.125)
P	(0.280, 0.280, 0.280)	(0.384, 0.384, 0.384)

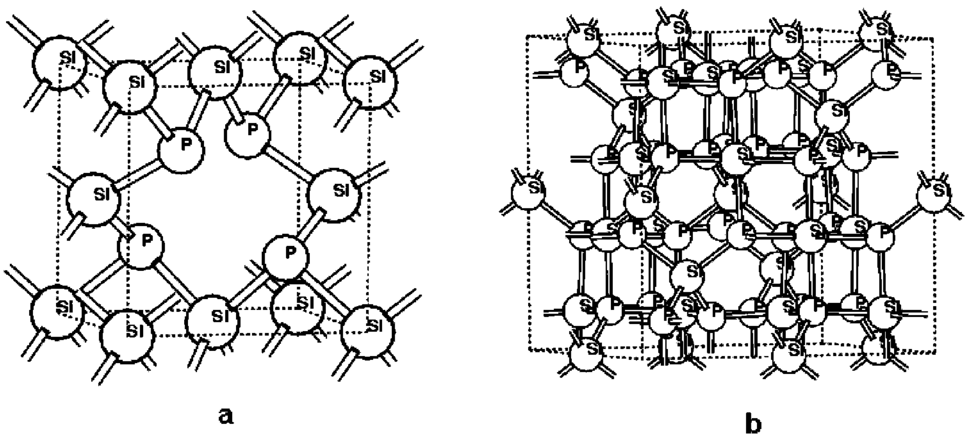

FIG. 2. Ball-stick model of (a) pseudocubic-Si_3P_4, (b) γ-Si_3P_4.

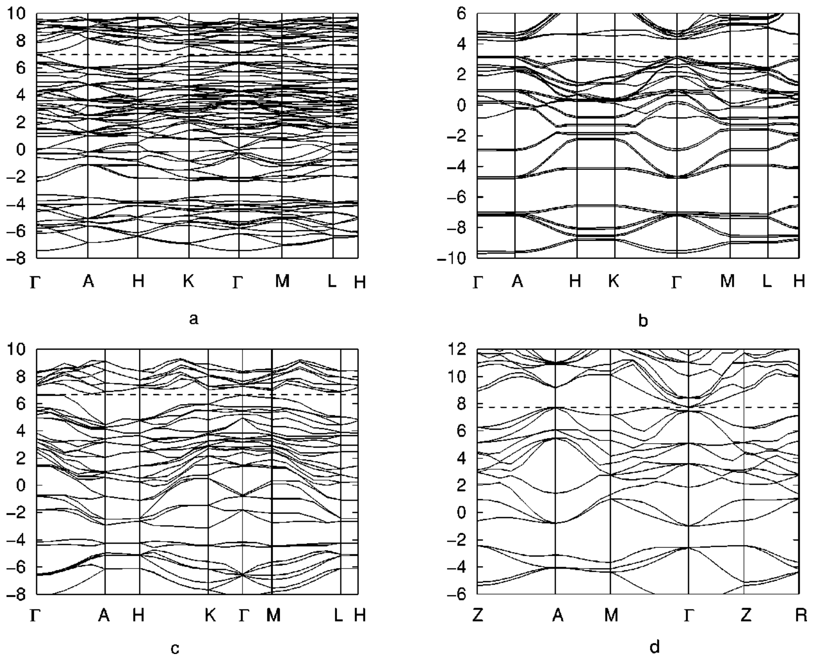

FIG. 3. Calculated band structure of (a) α-Si_3P_4, (b) graphitic-Si_3P_4, (c) $\beta1$-Si_3P_4, and (d) pseudocubic-Si_3P_4. The Fermi energy is indicated by the horizontal dashed line.

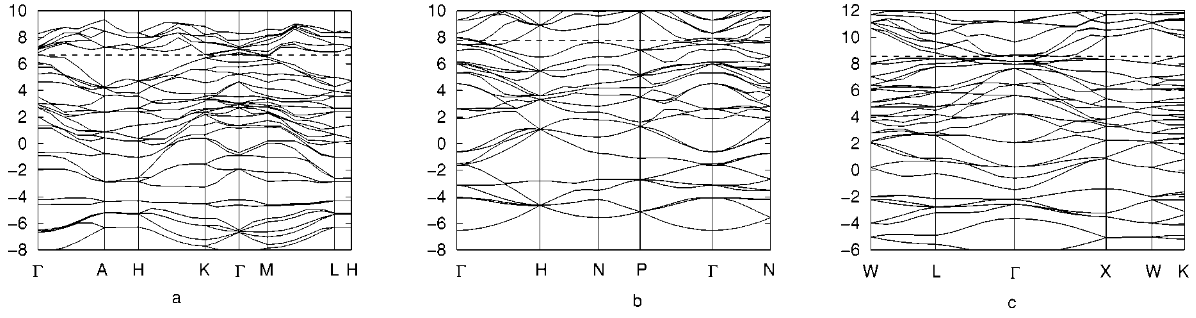

FIG. 4. Calculated band structure of (a) $\beta2$-Si_3P_4, (b) cubic-Si_3P_4, and (c) γ-Si_3P_4.

TABLE III. Calculated GGA equilibrium structural parameters and properties of various phases of Si_3P_4. ΔE_0 is the lowering of total energy per Si_3P_4 unit by GGA over that predicted by LDA at the equilibrium volume.

Structure	Pseudocubic	α	γ	Cubic	β_1	β_2	Graphitic
Lattice Parameter (Å)	$a=5.027$ $c=4.998$	$a=9.555$ $c=6.959$	$a=9.724$	$a=7.964$	$a=9.618$ $c=3.603$	$a=9.627$ $c=3.611$	$a=7.037$ $c=8.775$
B (GPa)	77	64	101	58	74	75	
E_0 (eV/Si_3P_4 unit)	-1050.87	-1050.21	-1049.95	-1049.73	-1049.68	-1049.56	-1047.86
ΔE_0 (eV/Si_3P_4 unit)	3.08	3.24	2.71	3.03	3.26	3.28	3.77
GGA band gap (eV)	0.134 (ind)	0.267 (dir)			0.279 (ind)		1.127 (ind)

only slightly smaller than that at the Γ point (0.984 eV). The valence-band maximum of β_1-Si_3P_4 is located at the Γ point but the minimum of its conduction band occurs at a point near A along the Γ-A direction, with an energy band gap of 0.082 eV. Pseudocubic-Si_3P_4 has nearly zero band gap between the A point of the valence band and the Γ point of the conduction band. From Fig. 4, we can see that the overlap between the valence and the conduction bands of β_2-, cubic-, and γ-Si_3P_4 are generally less than 1 eV. It is well known that LDA underestimates the band gap to a certain extent. It is possible that this overlap may be eliminated by other more accurate methods such as the GW method which improves the band gaps of boron nitride (BN), boron phosphide (BP), and boron arsenides (BA) by ~50%,[22] and that of β-C_3N_4 by ~100%.[23] Therefore it is possible that β_2-, cubic-, and γ-Si_3P_4 are narrow-gap semiconductors. Considering also the fact that the only structure with a relatively wide band gap, graphitic-Si_3P_4, is energetically less favorable and the remaining three semiconducting phases all have band gaps less than 0.2 eV, we can conclude that Si_3P_4 is likely a narrow gap semiconductor, rather than a wide gap semiconductor as expected.

While LDA performs very well for energetics of insulators and semiconductors, the generalized gradient approximation sometimes gives better agreement with experiment for simple metals and some transition metals. Here, we also carried our calculations using the parameter-free form of the exchange-correlation functional given by Perdew and Wang (GGA-PW91),[24] while keeping all other parameters the same as in the LDA calculations. The calculated results are listed in Table III. The GGA lattice constants and the band gaps are larger than the LDA results to a small extent. The equilibrium total energy and bulk moduli are a slightly smaller than the LDA results, which are expected. Unlike LDA, the GGA predicts that α-Si_3P_4 has a lower total energy and therefore more stable than γ-Si_3P_4. This, however, is not surprising since GGA has been observed to lower the total energy of a less dense structure more than a dense structure.[25–27]

DISCUSSION

C_3N_4 is a known superhard insulator. Its bulk modulus was predicted to be comparable to that of diamond.[13] Replacing C by Si in C_3N_4 results in Si_3N_4 which also has a wide band gap (4.6–5.5 eV) and a relatively high bulk modulus (256 GPa).[12] Ge_3N_4 was also investigated and were found to have similar properties as Si_3N_4.[14,15,28] However, anomalous properties were predicted for C_3P_4 which is obtained by substituting N with P in C_3N_4.[16] The pseudocubic phase of C_3P_4 is predicted to be exceptionally stable, with a relatively high bulk modulus and high density among the possible phases of C_3P_4.[16] Furthermore, C_3P_4 is very likely metallic.[16] In this study, we investigated the structure and properties of Si_3P_4 which can be obtained from C_3N_4 by replacing C by Si and

TABLE IV. Comparison of structures and properties of group-IV nitrides and group-IV phosphides.

	C_3N_4	Si_3N_4	Ge_3N_4	C_3P_4	Si_3P_4
Most stable phase	graphite[a]	β[c]	β[e]	Peudocubic[f]	Peudocubic[g]
Volume (Å^3/unit)	65.44[a]	73.0[d]	81.4[e]	69.0[f]	122.5[g]
Bulk modulus (GPa)	425[a]	256[d]	219[e]	203[f]	78[g]
Cohesive energy (eV/unit)	47.71[b] 40.75[c]	37.15[c]		42.6[f]	42.32[g]
LDA band-gap energy (eV)		3.2[c]	3.11[e]	<0[f]	<0.2[g]

[a] Reference 13.

[b] Reference 31, for β-C_3N_4.

[c] Reference 30. The cohesive energies of Si_3N_4 given here is consistently lower. A refined calculation was done for C_3N_4 in Ref. 31.

[d] Experimental value.

[e] Reference 15.

[f] Reference 16.

[g] This work.

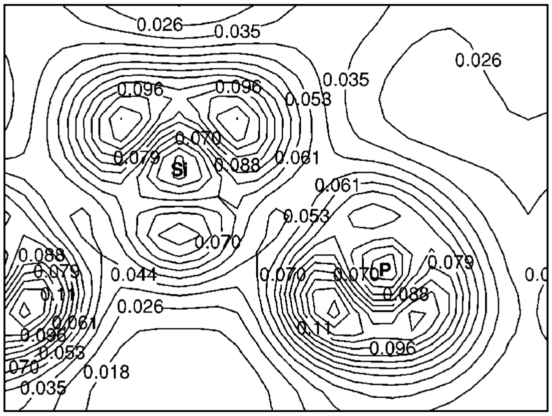

FIG. 5. Contour plot of electron density in the (101) plane of pseudocubic-Si$_3$P$_4$.

N by P simultaneously. From the results of this study, pseudocubic-Si$_3$P$_4$ is predicted to be the most energetically stable phase which is similar to C$_3$P$_4$. Si$_3$P$_4$ is softer compared to C$_3$N$_4$, Si$_3$N$_4$, Ge$_3$N$_4$, and C$_3$P$_4$ which is not unexpected. However, Si$_3$P$_4$ is likely a narrow gap semiconductor.

Similar to C$_3$P$_4$, Si$_3$P$_4$ is found to be in favor of sp^3 bonding, which is expected and explains the stability of pseudocubic-Si$_3$P$_4$. In pseudocubic-Si$_3$P$_4$, the Si-P-Si bond angle is 102.6°, which is slightly less than the ideal tetrahedral bond angle of 109.5°. The Si-P bond length is 2.25 Å, which is very close to the ideal tetrahedral bond length of 2.27 Å.[29] It is generally believed that the first-row elements, with localized $2p$ states, prefer sp^2 hybridization while sp^3 hybridization prevails as we move down the periodic table. Therefore it is not surprising that the most stable structure of Si$_3$P$_4$ is a tetrahedral structure. The Si-P bond length of α-Si$_3$P$_4$ is 2.218 Å within LDA and 2.216 Å within GGA, but the Si-P-Si bond angle is 107.9° within LDA and 109.2° within GGA. It seems that the P atom in α-Si$_3$P$_4$ within GGA is more likely to form sp^3 hybridization than within LDA. It is thus not surprising that GGA predicts an energetically more favorable α-Si$_3$P$_4$ than γ-Si$_3$P$_4$. Accurate thermodynamic data may be needed to clarify the relative stability of these two phases of Si$_3$P$_4$.

Pseudocubic-Si$_3$P$_4$ also has a relatively large cohesive energy which is comparable to that of C$_3$P$_4$ and is only slightly smaller than those of C$_3$N$_4$ and Si$_3$N$_4$ (see Table IV). It is noted that the cohesive energy of C$_3$N$_4$ given in Ref. 30 is much lower than that given by a refined calculation in Ref. 31. A similar underestimation can be expected for the cohesive energy of Si$_3$N$_4$ in Ref. 30, and a more accurate calculation such as that used in Ref. 31 would yield a cohesive energy a few eV per formula unit higher for Si$_3$N$_4$ than that given in Ref. 30 (37.15 eV per formula unit). The strong binding of Si$_3$P$_4$ could be the result of covalent bonding in pseudocubic-Si$_3$P$_4$. In Fig. 5, we show the electron density corresponding to the three top-most valence bands for pseudocubic-Si$_3$P$_4$ in the (101) plane. It is clear that the Si-P bond is of covalent nature, but the electrons are less localized compared to that in C$_3$N$_4$ and C$_3$P$_4$. It is interesting to note that sp^2 hybridization of N dominates in β-Si$_3$N$_4$, and the lowest energy structure of Si$_3$N$_4$ is hexagonal, but C$_3$P$_4$ prefers a tetrahedral structure. This suggests that substitution of N in C$_3$N$_4$ by another group-V element such as P changes its bonding nature from sp^2 hybridization to sp^3, leading to different structural and electronic properties of the compounds, while substitution of C by another group-IV element results in a compound of similar properties.

Based on the empirical model for the bulk moduli of tetrahedrally-bonded covalent solids in the diamond and zinc-blende structures,[32,33] the bulk modulus of Si$_3$P$_4$ is expected to be about 100 GPa. The calculated bulk moduli, however, are generally smaller than predicted. The only exception is the γ phase, which is known to be a high-pressure phase for this type of compounds.[21] The bulk modulus of pseudocubic-Si$_3$P$_4$ is about 78 GPa. The smaller bulk moduli of Si$_3$P$_4$, compared to those of C$_3$N$_4$, Si$_3$N$_4$, Ge$_3$N$_4$, and C$_3$P$_4$ is expected, since the atom sizes and therefore the bond lengths and equilibrium volume per formula unit are much larger in Si$_3$P$_4$ (see Table IV).

Electronegativity may play an important role in determining electronic properties of group-IV nitrides and group-IV phosphides.[16] The electronegativities of N, C, P, and Si are 3.00, 2.50, 1.64, and 1.41, respectively.[34] Since the electronegativity describes the ability of an atom to attract electrons to itself, it is expected that the valence electrons in Si-N or C-N bonds will be attracted strongly by the N atoms which was confirmed by first-principles electronic structure calculation.[30] Both C$_3$N$_4$ and Si$_3$N$_4$ are wide gap insulators. The charge density for C$_3$N$_4$ was found to be covalent in nature, with the charge weighted towards the N sites. The charge density for Si$_3$N$_4$ exhibits much more ionic character and resembles more closely to those found in III–V systems due to the large difference in electronegativities of Si and N. On the other hand, P has a smaller electronegativity and therefore more willing to donate electrons to C in C$_3$P$_4$ which is believed to be the reason for the metallic character of C$_3$P$_4$. In the case of Si-P bond, since the difference in electronegativities of the two atoms is very small, the bonding can be expected to be covalent. This is seen in Fig. 5. However, the valence electrons filling the top valence bands are not strongly localized.

CONCLUSION

In summary, using first-principles pseudopotential calculations, we have investigated the structural and electronic properties of Si$_3$P$_4$. We found that pseudocubic-Si$_3$P$_4$ is the most energetically favored as well as mechanically stable. Si$_3$P$_4$ has a relatively low bulk modulus and is expected to be a narrow gap semiconductor. Although Si$_3$P$_4$ can be obtained from Si$_3$N$_4$ by substitution of N with P or from C$_3$P$_4$ by substitution of C with Si, Si$_3$P$_4$ behaves more like C$_3$P$_4$ rather than Si$_3$N$_4$. The present work further demonstrates distinct properties of group-IV phosphides and group-IV nitrides.

*Corresponding author. Email address: phyfyp@nus.edu.sg

[1] K. Sasaki, M. M. Rahman, and S. Fukazawa, IEEE Electron Device Lett. **6**, 311 (1985).

[2] X.-H. Li, J. R. A. Carlesson, M. Johansson, B. Ekstrom, S. F. Gong, and H. T. G. Henzell, Appl. Phys. Lett. **61**, 1316 (1992).

[3] A. V. Dvurechenskii, I. A. Ryazantsev, L. S. Smirnov, H. Klose, and M. Rieth, Phys. Status Solidi A **79**, 83 (1983).

[4] X.-H. Li, J. R. A. Carlesson, S. F. Gong, and H. T. G. Hentzell, J. Appl. Phys. **76**, 5179 (1994).

[5] J. R. A. Carlesson, L. D. Madsen, M. P. Johansson, L. Hultman, X.-H. Li, H. T. G. Hentzell, and L. R. Wallenberg, J. Vac. Sci. Technol. A **15**, 394 (1997).

[6] J. R. A. Carlesson, L. Clevenger, L. D. Madsen, L. Hultman, X.-H. Li, J. Jordan-Sweet, C. Lavoie, R. A. Roy, C. Cabral, Jr., G. Morales, K. L. Ludwig, G. B. Stephenson, and H. T. G. Hentzell, Philos. Mag. B **75**, 363 (1997).

[7] X.-H. Li, J. R. A. Carlesson, S. F. Gong, H. T. G. Hentzell, and B. Liedberg, J. Appl. Phys. **77**, 301 (1995).

[8] J. R. A. Carlesson, J.-E. Sundgren, L. D. Madsen, X.-H. Li, and H. T. G. Hentzell, Thin Solid Films **300**, 51 (1997).

[9] A. G. Baboul and H. B. Schlegel, J. Am. Chem. Soc. **118**, 8444 (1996).

[10] P. Hohenberg and W. Kohn, Phys. Rev. **136**, A864 (1964).

[11] W. Kohn and L. J. Sham, Phys. Rev. **140**, A1133 (1965).

[12] W. Y. Ching, L. Ouyang, and J. D. Gale, Phys. Rev. B **61**, 8696 (2000).

[13] D. M. Teter and R. J. Hemley, Science **271**, 53 (1996).

[14] J. Dong, O. F. Sankey, S. K. Deb, G. Wolf, and P. F. Mcmillan, Phys. Rev. B **61**, 11 979 (2000).

[15] B. Molina and L. E. Sansores, Int. J. Quantum Chem. **80**, 249 (2000).

[16] A. T. L. Lim, Y. P. Feng, and J. C. Zheng, Int. J. Mod. Phys. B **16**, 1101 (2002); A. T. L. Lim, Y. P. Feng, and J. C. Zheng, Mater. Sci. Eng., B **99**, 527 (2003).

[17] M. C. Payne, M. P. Teter, D. C. Allan, T. A. Arias, and J. D. Joannopoulos, Rev. Mod. Phys. **64**, 1045 (1992).

[18] V. Milman, B. Winkler, J. A. White, C. J. Pickard, M. C. Payne, E. V. Akhmatskaya, and R. H. Nobes, Int. J. Quantum Chem. **77**, 895 (2000).

[19] D. Vanderbilt, Phys. Rev. B **41**, 7892 (1990).

[20] H. J. Monkhorst and J. D. Pack, Phys. Rev. B **13**, 5188 (1976).

[21] Andreas Zerr, Gerhard Miehe, George Serghiou, Marcus Schwarz, Edwin Kroke, Ralf Riedel, Hartmut Fue, Peter Kroll, and Reinhard Boehler, Nature (London) **400**, 340 (1999).

[22] M. P. Surh, S. G. Louie, and M. L. Cohen, Phys. Rev. B **43**, 9126 (1991).

[23] J. L. Corkill and M. L. Cohen, Phys. Rev. B **48**, 17 622 (1993).

[24] J. P. Perdew and Y. Wang, Phys. Rev. B **45**, 13 244 (1992).

[25] J. P. Perdew, J. A. Chevary, S. H. Vosko, K. A. Jackson, M. R. Pederson, D. J. Singh, and C. Fiolhais, Phys. Rev. B **46**, 6671 (1992).

[26] D. R. Hamann, Phys. Rev. Lett. **76**, 660 (1996).

[27] A. Janotti, S.-H. Wei, and D. J. Singh, Phys. Rev. B **64**, 174107 (2001).

[28] Y. Duan, K. Zhang, and X. Xie, Phys. Status Solidi B **200**, 499 (1997).

[29] C. Kettel, *Introduction to Solid State Physics*, 7th edition (Wiley, New York, 1996).

[30] A. Y. Liu and M. L. Cohen, Phys. Rev. B **41**, 10 727 (1990).

[31] A. Y. Liu and R. M. Wentzcovitch, Phys. Rev. B **50**, 10 362 (1994).

[32] M. L. Cohen, Phys. Rev. B **32**, 7988 (1985).

[33] C-M. Sung and M. Sung, Mater. Chem. Phys. **43**, 1 (1996).

[34] J. C. Phillips, *Bonds and Bands in Semiconductors* (Academic Press, New York, 1973).